Quantum Electronics **27** (10) 892 – 896 (1997)

PACS numbers: 42.55.Ah; 42.60.Mi

Phase and amplitude dynamics of the TEM_{10} and TEM_{01} modes in a class-B laser

D V Skryabin, A G Vladimirov, A M Radin

Abstract. Dynamics of generation of two transverse modes in a class-B laser is investigated theoretically. The bifurcation mechanisms of excitation of steady-state, periodic, and chaotic regimes are studied. It is shown that dynamic transverse structures can either rotate continuously or can oscillate about the optic axis.

The present investigation is a continuation of earlier work [1] in which the equations of generation of three transverse modes TEM_{00}, TEM_{10}, and TEM_{01} in a class-B laser were derived and investigated. Here, we shall study in detail the special case when the TEM_{00} fundamental mode is suppressed. This situation had been achieved experimentally on many occasions [2 – 8] and was investigated theoretically [2, 9, 10]. The published results demonstrate that astigmatism-induced splitting of the TEM_{10} and TEM_{01} mode frequencies has a significant influence on laser dynamics. A special feature of our investigation is a study of both amplitude and phase dynamics. In particular, we shall show that the phase effects lead to two types of motion of transverse structures: these structures may either rotate continuously or can oscillate about the optic axis.

If the amplitudes F_{10} and F_{01} of the TEM_{10} and TEM_{01} modes, varying slowly with time, are replaced with the functions

$$F_{\pm} = F_{10}\exp\left[\mathrm{i}\frac{(\omega_{10}-\omega_{01})t}{2}\right] \mp \mathrm{i}F_{01}\exp\left[\mathrm{i}\frac{(\omega_{01}-\omega_{10})t}{2}\right], \quad (1)$$

scaling transformations modify the mode-generation equations to

$$\begin{aligned}
&\partial_\tau F_+ = (1-\mathrm{i}\Delta)(F_+N_0 + F_-N_2) + \mathrm{i}R\exp(\mathrm{i}\psi)F_- \ ,\\
&\partial_\tau F_- = (1-\mathrm{i}\Delta)(F_-N_0 + F_+N_2^*) + \mathrm{i}R\exp(\mathrm{i}\psi)F_+ \ ,\\
&\partial_\tau N_0 = 1-\gamma N_0 - |F_+|^2 - |F_-|^2 \ ,\\
&\partial_\tau N_2 = -\gamma N_2 - F_+F_-^* \ .
\end{aligned} \quad (2)$$

D V Skryabin Physics and Applied Physics Department, University of Strathclyde, John Anderson Building, 107 Rottenrow, Glasgow G4 0NG, UK, fax: (44) 141 5522891, e-mail: dmitry@phys.strath.ac.uk;
A G Vladimirov Quantum Electronics Division, Scientific-Research Institute of Physics at the St Petersburg State University, Ul'yanovskaya ul. 1, Peterhof, 198904 St Petersburg (current address: Optique Nonlinéaire Théorique, Université Libre de Bruxelles, B-1050 Bruxelles, Belgium, fax: (32) 2 6505824, e-mail: avladimi@ulb.ac.be);
A M Radin Applied Mathematics Division, Refrigeration Academy, ul. Lomonosova 9, 191002 St Petersburg

Received 21 June 1996; revision received 26 March 1997
Kvantovaya Elektronika **24** (10) 918 – 922 (1997)
Translated by A Tybulewicz

Here, ω_{10} and ω_{01} are the eigenfrequencies of the TEM_{10} and TEM_{01} modes; $R\cos\psi$ and $R\sin\psi$ represent, respectively, the frequency difference and the loss difference for the TEM_{10} and TEM_{01} modes, such that if $\psi = 0$, then $R = |\omega_{10} - \omega_{01}|/2$; $F_{\pm} = \rho\exp(-\rho^2 \pm \mathrm{i}\vartheta)$ are the Laguerre–Gauss mode amplitudes; ρ is the distance from the beam axis, normalised to the beam radius; ϑ is the polar angle; N_0 and N_2 are the zeroth and second angular harmonics of the population inversion described by formulas (2) and (5) in Ref. [1]; Δ is the dimensionless detuning from the line centre in the absence of frequency splitting; $\gamma = (\gamma_\parallel/\varkappa\varepsilon)^{1/2}$; $\gamma_\parallel$ is the inversion decay constant; $\varkappa$ represents the cavity losses; ε is the excess of the pumping rate above the threshold, normalised to $\varkappa$; τ is the dimensionless time.

The system of equations (2) in invariant under the $F_{\pm} \to F_{\mp}\mathrm{e}^{\mathrm{i}\Theta}$ transformation. It is therefore convenient to introduce variables which are invariant under this transformation:

$$\begin{aligned}
&x_1 = 2\,\mathrm{Re}N_2 \ , \quad x_2 = 2\mathrm{Im}N_2 \ , \quad x_3 = N_0 \ ,\\
&x_4 = |E_-||E_+|\cos\mu \ , \quad x_5 = |E_-||E_+|\sin\mu \ ,\\
&x_6 = |E_+|^2 - |E_-|^2 \ , \quad x_7 = |E_+|^2 + |E_-|^2 \ .
\end{aligned} \quad (3)$$

Here, $\mu = \arg F_+ - \arg F_-$. In terms of these new variables, the system of equations (2) becomes

$$\begin{aligned}
&\partial_\tau x_1 = -\gamma x_1 - x_4 \ , \quad \partial_\tau x_2 = -\gamma x_2 + x_5 \ ,\\
&\partial_\tau x_3 = -\gamma x_3 - x_7 + 1 \ ,\\
&\partial_\tau x_4 = -2x_7R\sin\psi + x_7x_1 + \Delta x_6x_2 + 2x_4x_3 \ ,\\
&\partial_\tau x_5 = 2x_6R\cos\psi - x_7x_2 + \Delta x_6x_1 + 2x_5x_3 \ ,\\
&\partial_\tau x_6 = -2x_5R\cos\psi + 2x_6x_3 - \Delta(x_5x_1 + x_4x_2) \ ,\\
&\partial_\tau x_7 = -2x_4R\sin\psi + 2x_7x_3 - x_5x_2 + x_4x_1 \ .
\end{aligned} \quad (4)$$

It is important for further analysis that the system of equations (4) is invariant under the transformation

$$(x_1, x_2, x_3, x_4, x_5, x_6, x_7) \to (x_1, -x_2, x_3, x_4, -x_5, -x_6, x_7) \ . \quad (5)$$

In addition to the zeroth solution, the above system has six steady-state solutions. There is a pair of solutions of the standing-wave type with $|F_+|^2 = |F_-|^2$:

$$\begin{aligned}
&x_7 = \frac{2}{3}(1 \pm \gamma R\sin\psi) \ , \quad x_6 = x_5 = x_2 = 0 \ ,\\
&x_4 = \frac{2}{3}(\mp 1 - \gamma R\sin\psi) \ , \quad x_3 = \frac{1-x_7}{\gamma} \ , \ x_1 = \frac{-x_4}{\gamma} \ .
\end{aligned} \quad (6)$$

The upper and the lower signs correspond to the TEM_{01} and TEM_{10} modes, respectively. Moreover, there are four

more travelling-wave solutions with $|F_+|^2 > |F_-|^2$ and $|F_+|^2 < |F_-|^2$:

$$x_7 = \frac{1}{2f_2}\left[-f_1 \pm (f_1^2 - 4f_2f_0)^{1/2}\right], \quad x_6 = \frac{\pm 1}{(1-x_7)\Delta^2} \times \{9x_7^3 - 21x_7^2 + [R^2\gamma^2(\Delta \sin 2\psi + 6\cos^2\psi) + 16]x_7 - 4(1 + R^2\gamma^2\cos^2\psi)]^{1/2}, \quad x_5 = \frac{x_6(1-x_7)}{\gamma R\cos\psi},$$

$$x_4 = \frac{3x_7^2 - 5x_7 + 2\gamma^2R^2\cos^2\psi + 2}{\gamma\Delta R\cos\psi}, \qquad (7)$$

$$x_3 = \frac{1-x_7}{\gamma}, \quad x_2 = \frac{x_5}{\gamma}, \; x_1 = -\frac{x_4}{\gamma},$$

where

$$f_0 = -2(R^2\gamma^2\cos^2\psi + 1)(\Delta\sin\psi + \cos\psi),$$
$$f_1 = 4\Delta\sin\psi + (\Delta^2 + 5)\cos\psi,$$
$$f_2 = -\Delta\sin\psi - (\Delta^2 + 3)\cos\psi.$$

The minus and plus signs in the expression (3) for the total intensity x_7 of counterpropagating waves correspond to a pair of travelling-wave regimes which will be denoted by TW_+ and TW_- (TW1 and TW2). Reversal of the sign in front of the difference x_6 between the counterpropagating wave intensities means replacement of TW_+ with TW_- or of TW1 with TW2. The singularity of x_4 and x_6 at $\Delta = 0$ disappears after substitution of the explicit expression for x_7. The travelling-wave regimes exist only if $f_1^2 > 4f_2f_0$. The TW_+ (TW_-) solution merges with TW1 (TW2) at a saddle–node bifurcation defined by the equality $f_1^2 = 4f_2f_0$. The TW1 and TW2 are always unstable, whereas TW_+ and TW_- exist in a wide range of parameters and can experience a Hopf bifurcation.

The bifurcation diagram for the steady-state solutions in the (γ, R) plane is given in Fig. 1a for $\Delta = 0$ and $\psi = \pi/3$. The TEM_{01} mode is stable in the region DHFED and the solutions TW_+ and TW_- are stable in the region ABCDHKA. The BHF (DHM) curve corresponds to a supercritical Hopf bifurcation (fork) of the TEM_{01} mode and the HK curve corresponds to a subcritical Hopf bifurcation of the solutions TW_+ and TW_-. When astigmatism is sufficiently strong (i.e. when R is greater than a certain critical value R_{cr}) and γ is small, all the regimes of generation of constant-intensity modes are unstable. Intersection of the HK curve in Fig. 1a with the abscissa gives R_{cr}. An analytic expression for this critical value is given in Ref. [11].

The bifurcation diagram in the (Δ, γ) plane is shown in Fig. 1b for the $R < R_{cr}$ case. The TEM_{01} mode is stable in region FZTLKHGF and the solutions TW_+ and TW_- are stable in region ARDEFZGHKVA. The DRAVK (BPTL) curve corresponds to a Hopf bifurcation of the TW_+ and TW_- (TEM_{01}) solutions. These bifurcations are supercritical (subcritical) on the BPTL, DR, and VK (RAV) lines. The FZ (ZTNM) curve corresponds to a supercritical (subcritical) bifurcation of the fork of the TEM_{01} mode, and the ZG curve corresponds to a saddle–node bifurcation where the solutions TW_+ and TW1 (TW_- and TW2) merge and disappear. The RS and XY curves correspond, respectively, to a saddle–node bifurcation of limit cycles and a bifurcation of a limit cycle into a quasiperiodic attractor. All the bifurcation curves are based on numerical calculations. The Hopf bifurcation and fork lines for standing-wave regimes and the saddle–node bifurcation line for travelling waves were additionally calculated analytically. Numerical estimates and a discussion of the dimensionless parameters used here can be found in Ref. [1].

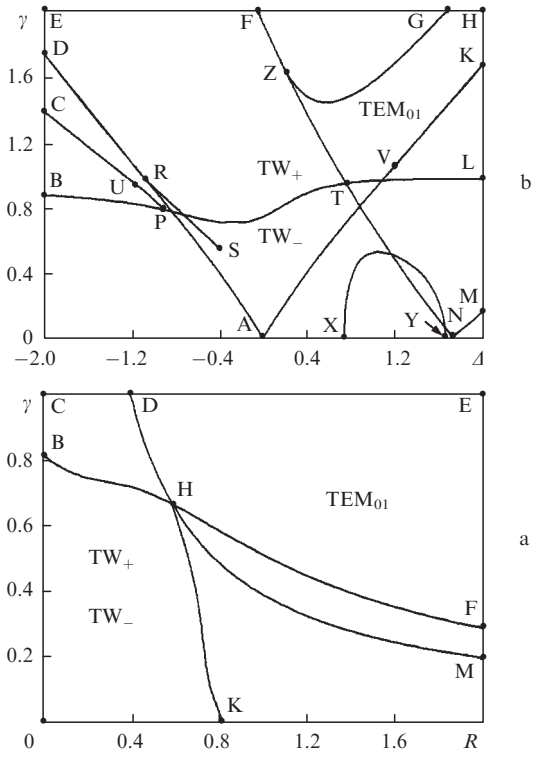

Figure 1. Bifurcation diagrams of the system of equations (4) obtained for $\Delta = 0$, $\psi = \pi/3$ (a) and $R = 0.2$, $\psi = \pi/3$ (b).

We shall now describe dynamic structures which appear as a result of supercritical Hopf bifurcations of steady-state solutions. The intensity distribution in a transverse section of a laser beam is

$$I(\rho, \vartheta, t) = \rho^2\left[|F_+|^2 + |F_-|^2 + 2|F_+||F_-|\cos(2\vartheta + \mu)\right]\exp(-\rho^2). \qquad (8)$$

If $F_+F_- \neq 0$, then for a given value of ρ, the above intensity has a minimum at

$$\vartheta = \vartheta_{min} = (-\mu \pm \pi)/2. \qquad (9)$$

The phase difference μ is a function of time for periodic solutions of the system of equations (4). Consequently, the angular velocity of rotation of the intensity minimum is $\partial_\tau\vartheta_{min} = -\partial_\tau\mu/2$. If the projection of a cycle onto the (x_4, x_5) phase plane includes the point $x_4 = x_5 = 0$ ($x_4 \propto \cos\mu$, $x_5 \propto \sin\mu$), then μ increases or decreases continuously, depending on the direction in which a cycle is traversed as a function of time. For such cycles, the phase difference μ can be written in the form

$$\mu(\tau) = \pm\frac{2\pi m\tau}{T} + \mu_d(\tau). \qquad (10)$$

Here, T is the period of a limit cycle, i.e. the period of the intensity pulsations; m is the number of complete rotations around the point $x_4 = x_5 = 0$ during one period; μ_d is a periodic function of time with the period T; $\mu_d(\tau) = \mu_d(\tau + T)$. The

selection of the plus or minus sign in expression (10) depends on the direction along which a limit cycle is traversed.

In this case the quantity $\vartheta_{\min}$ is a continuously rising or falling function of time and, therefore, an intensity minimum rotates continuously clockwise or anticlockwise. The total angle of rotation in the time $\tau = nT$ (n is an integer) is $\pm 2\pi nm$. If the projection of a limit cycle onto the (x_4, x_5) plane does not include the point $x_4 = x_5 = 0$, then μ is a bounded periodic function of time: $\mu(\tau) = \mu_d(\tau)$. In this case the intensity minimum oscillates clockwise or anticlockwise in a finite interval of the polar angles.

The investigated system of equations is invariant under the reflection transformation described by expression (5). Therefore, all the nonvariant solutions exist in pairs. One of these solutions is transformed into the other by the reflection transformation. Consequently, each stable regime with a continuously rising phase difference $\mu(\tau)$ always corresponds to a stable regime with a continuously falling $\mu(\tau)$.

Projections of the limit cycles that appear after supercritical Hopf bifurcations of the solutions TW_+ and TW_- do not include the point $x_4 = x_5 = 0$ and, therefore, they correspond to transverse structures which oscillate in a finite interval $\delta\vartheta$ of the polar angles. As $|\Delta|$ is increased, the dimensions of both cycles increase and the point $x_4 = x_5 = 0$ is now included in these projections. Transverse structures are continuously transformed from oscillation to rotation about the optic axis. Solutions of the standing-wave type are invariant under the reflection transformation described by expression (5) and their Hopf bifurcations create invariant cycles. Symmetric cycles cannot include the point $x_4 = x_5 = 0$ and, therefore, they always correspond to oscillating transverse structures.

An orbit, which is homoclinic relative to an unstable steady-state solution corresponding to generation of the TEM_{01} mode, exists along the CUP line (Fig. 1b). This solution is of the saddle–focus type. Shil'nikov [12] showed that, if there is a loop which is homoclinic relative to a saddle–focus (this saddle–focus is a steady-state solution with the eigenvalues $\lambda_1, -\lambda_2 + i\omega$, $\lambda_1\lambda_2 > 0$; the real parts of the remaining eigenvalues are negative and their moduli exceed $|\lambda_{1,2}|$) and the condition $|\lambda_2/\lambda_1| < 1$ is satisfied, then for similar values of the parameters in the vicinity of this saddle–focus there is a chaotic set of solutions. The Shil'nikov conditions are satisfied in a segment labelled UP. To the right of the CU line there is a pair of asymmetric [under the transformation described by expression (5)] stable cycles, whereas to the left there is a stable symmetric cycle. Fig. 2 shows chaotic dependences of the mode intensities and of the difference between their phases μ on the dimensionless time τ, obtained for parameters close to those at the point P (Fig. 1b).

We shall now describe bifurcations of the system of equations (4) which involve an increase in the detuning for $R = 0.2$, i.e. for $R < R_{cr}$. At the point R the first Lyapunov coefficient vanishes and a supercritical Hopf bifurcation of solutions TW_+ and TW_- changes to a subcritical one. The bifurcation line RS, on which the stable and unstable limit cycles merge [13], begins at this point. These stable and unstable cycles are not symmetric relative to the reflection transformation described by expression (5). Therefore, there is a pair of stable cycles and a pair of unstable ones. The projection of the stable cycles onto the (x_4, x_5) plane includes the origin of the coordinate system. Consequently, these cycles correspond to rotating transverse structures. A pair of stable cycles experiences a cascade of period-doubling

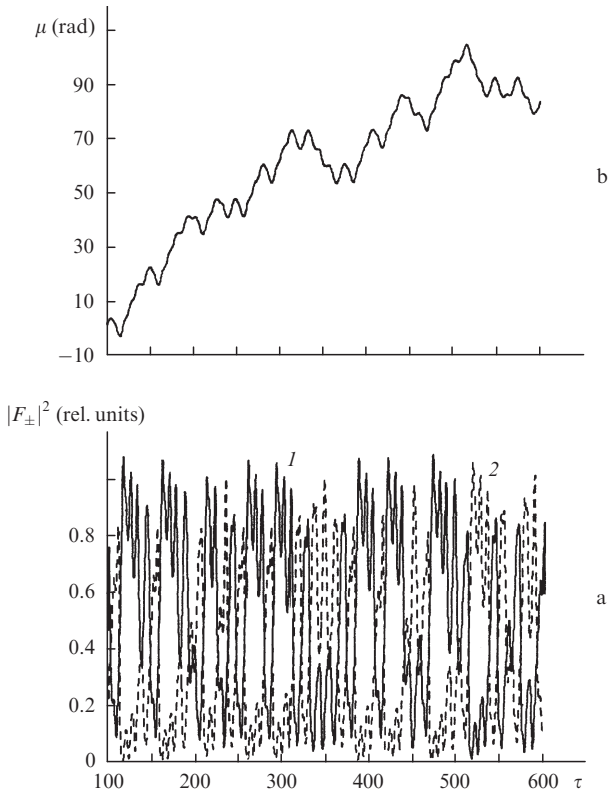

Figure 2. Time dependences of the intensities $|F_+|^2$ (*1*) and $|F_-|^2$ (*2*) (a), and also of the phase differences μ (b) in the vicinity of the point P (Fig. 1b); $\Delta = -1.066$, $\gamma = 0.89$, $\psi = \pi/3$, $R = 0.2$.

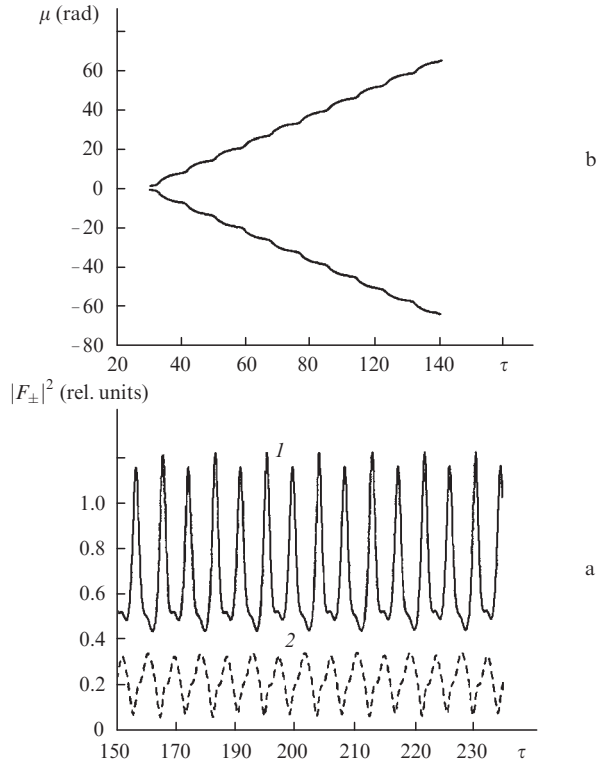

Figure 3. Time dependences of the intensities $|F_+|^2$ (*1*) and $|F_-|^2$ (*2*) (a), and also of the phase differences μ (b) in the vicinity of the point P (Fig. 1a); $\Delta = -0.62$, $\gamma = 0.5$, $\psi = \pi/3$, $R = 0.2$.

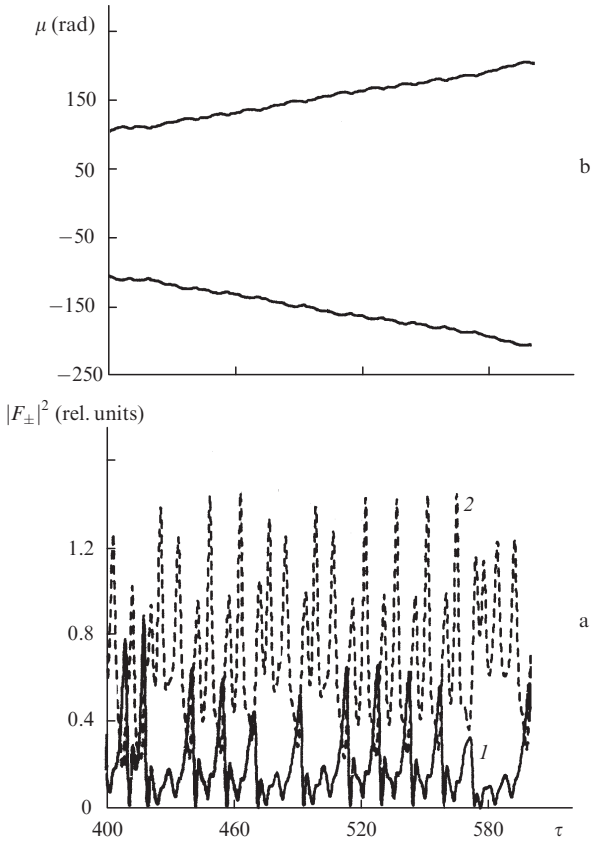

Figure 4. Time dependences of the intensities $|F_+|^2$ (*1*) and $|F_-|^2$ (*2*) (a), and also of the phase differences μ (b) in the vicinity of the point P (Fig. 1a); $\Delta = -0.632$, $\gamma = 0.5$, $\psi = \pi/3$, $R = 0.2$.

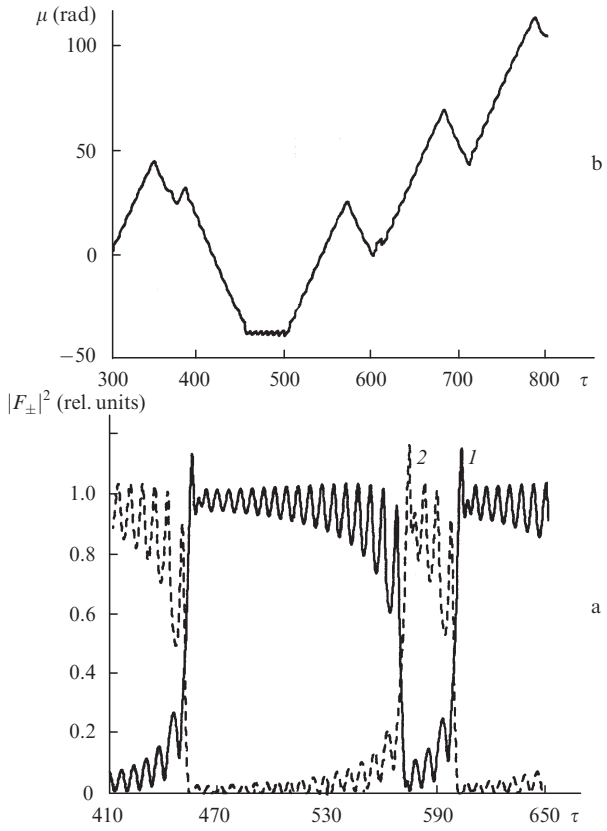

Figure 5. Time dependences of the intensities $|F_+|^2$ (*1*) and $|F_-|^2$ (*2*) (a), and also of the phase differences μ (b) in the vicinity of the point P (Fig. 1a); $\Delta = -0.65$, $\gamma = 0.5$, $\psi = \pi/3$, $R = 0.2$.

bifurcations as a result of a shift in the direction of the negative detuning.

Fig. 3 gives the mode intensities of one of the doubled limit cycles and the difference between the phases of these modes for both cycles. A sequence of doubling bifurcations gives rise to a pair of bistable chaotic attractors. Fig. 4a demonstrates chaotic pulsations of the mode intensities corresponding to one of these attractors. The continuously rising and the continuously falling differences between the mode phases, corresponding to the two attractors, are plotted in Fig. 4b.

As the detuning increases, chaotic switching between the attractor pair begins (Fig. 5). The horizontal plateau in Fig. 5b means that a phase path not containing the point $x_4 = x_5 = 0$ is stabilised temporarily. A further increase in the detuning induces an opposite period-doubling cascade, which terminates in a region of periodic generation in the vicinity of $\Delta = -1$. In this region a pair of asymmetric limit cycles that do not include the point $x_4 = x_5 = 0$ is stable. Next, following a chaotic region (corresponding to the detuning interval from about -1 to -1.5), a pair of asymmetric limit cycles that do not include the point $x_4 = x_5 = 0$ is again stable.

A supercritical Hopf bifurcation of a stable standing wave (line TL in Fig. 1b) exists for the positive detuning. A shift out of the region of stability of the travelling-wave regime in the direction of the positive detuning gives rise to an initial bifurcation scenario similar to that shown in Figs 3–5. However, a chaotic region is followed by a symmetric limit cycle. This limit cycle experiences in its turn a Hopf bifurcation on the XY line and the result is a quasiperiodic attractor.

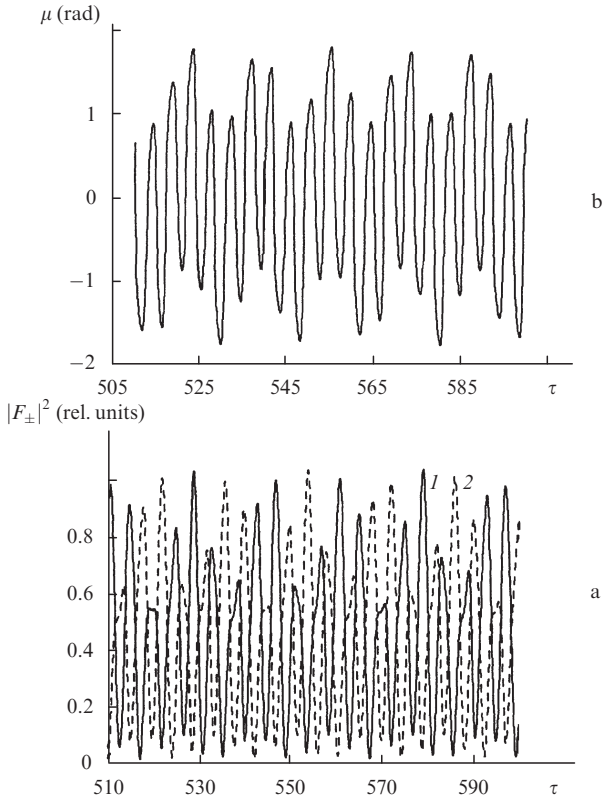

Figure 6. Time dependences of the intensities $|F_+|^2$ (*1*) and $|F_-|^2$ (*2*) (a), and also of the phase differences μ (b) in the vicinity of the point P (Fig. 1a); $\Delta = 1.2$, $\gamma = 0.5$, $\psi = \pi/3$, $R = 0.2$.

The corresponding intensities and the difference between the phases of the counterpropagating waves are given in Fig. 6.

To summarise, we analysed bifurcation mechanisms of the loss of stability of all the steady-state regimes which are possible in class-B lasers generating a pair of transverse modes TEM_{10} and TEM_{01}. It was found that the appearance of chaotic generation regimes is possible through a sequence of period-doubling bifurcations and by destruction of a separatrix loop. The feasibility of existence of dynamic transverse structures, rotating continuously about the optic axis or oscillating in a finite interval of the polar angles, was demonstrated and ways of appearance of such structures were discussed.

The system of equations (2) is identical with the system describing generation of counterpropagating waves in a ring class-B laser (as discussed in a review [11]). Then, $R\exp(i\psi)$ is a coefficient representing coupling of counterpropagating waves via backscattering and μ is the difference between the phases of these counterpropagating waves. We thus demonstrated that a ring laser with equivalent counterpropagating directions of the round trip may support regimes with a nonzero frequency of the counterpropagating wave beats. Such regimes were predicted earlier only for class-B lasers with inequivalent, for example because of the phase nonreciprocity, directions of counterpropagating waves in a round trip. Similar regimes were investigated by us recently for ring class-A lasers [14, 15].

References

1. Vladimirov A G, Skryabin D V *Kvantovaya Elektron. (Moscow)* **24** 913 (1997) [*Quantum Electron.* **27** ??? (1997)]
2. Boscolo I, Lugiato L A, Prati F, et al. *Opt. Commun.* **115** 379 (1995)
3. Green C, Mindlin G B, D'Angelo E J, et al. *Phys. Rev. Lett.* **65** 3124 (1990)
4. Coates A B, Weiss C O, Green C, et al. *Phys. Rev. A* **49** 1452 (1994)
5. Tamm C *Phys. Rev. A* **38** 5960 (1988)
6. Tang D Y, Heckenberg N R, Weiss C O *Opt. Commun.* **114** 95 (1995)
7. Arecchi F T, Giacomelli G, Ramazza P L, Residori S *Phys. Rev. Lett.* **65** 2531 (1990)
8. Hennequin D, Dambly L, Dangoisse D, Glorieux P *J. Opt. Soc. Am. B* **11** 676 (1994)
9. López-Ruiz R, Mindlin G B, Pérez-Garcia C, Tredicce J R *Phys. Rev. A* **49** 4916 (1994)
10. Brambilla M, Cattaneo M, Lugiato L A, et al. *Phys. Rev. A* **49** 1427 (1994)
11. Kravtsov N V, Lariontsev E G *Kvantovaya Elektron. (Moscow)* **21** 903 (1994) [*Quantum Electron.* **24** 841 (1994)]
12. Shil'nikov L P *Dokl. Akad. Nauk SSSR* **164** 1242 (1965)
13. Guckenheimer J, Holmes P *Nonlinear Oscillations, Dynamical Systems, and Bifurcations of Vector Fields* (Berlin: Springer, 1983)
14. Skryabin D V, Vladimirov A G, Radin A M *Opt. Commun.* **116** 109 (1995)
15. Skryabin D V, Vladimirov A G, Radin A M *Opt. Spektrosk.* **78** 989 (1995) [*Opt. Spectrosc.* **78** 896 (1995)]